

# Research on a Tubular Climbing Robot Induced by Tri-tube Soft Actuators

Long Li, Peifeng Ma, Yichen Jiang, Tao Jin, Tong Wu, Guangjie Yuan, and Yingzhong Tian\*

**Abstract-** In this paper, a pipe robot consisted of iris expansion mechanism and tri-tube soft actuators, which simulates insect crawling mode, is proposed. We used 3D-printing technology to fabricate the main structure of the robot. For displaying the detail working mechanism, the movement process diagram has been proposed. In order to identify the working ability, we investigated the operation space of the guiding mechanism based on equal continuous hypothesis and the adhesive output of the iris mechanism. The related performance experiments have been carried out to verify the analysis as well. Our results showed that the robot fixed by iris mechanism to the pipe could adapt to pipes with various diameters ranging from 80 to 120 mm (about 1.5 times as its original size). The guiding mechanism composed of three hoses driven by motors was easy to bend 90 degrees, which satisfied the curved pipe environments. The biggest characteristic of our robot is the flexible structure and adhesive methods, which gets rid of the limitation of air source and air pipe to the robot.

**Index Terms** – Soft robot, pipe climbing robots, iris mechanism, tri-tube soft actuators

## I. INTRODUCTION

In the field of robot development, how to realize the inspection, maintenance and cleaning of pipe mechanization is a big problem we are faced with [1]-[2]. Most robots are composed of rigid bodies, which have the disadvantages of poor flexibility and low environmental adaptability, and cannot adapt to the working environment where the direction of the bend changes [3]-[4]. However, the research on soft robots with good flexibility and strong environmental adaptability provides a new idea for the development of robots [5]-[6]. The design of flexible robots is mostly inspired by mollusks in nature. Their main body is mainly composed of elastic materials capable of withstanding large deformation, which can achieve continuous deformation and have a high degree of freedom [7]. By imitating the movement of mollusks [8], the soft robot can realize such movements as wriggling, wriggling, crawling and swimming [9].

For rigid crawling robot, it is difficult to turn and change the direction of movement. The rigid crawling robot does not have good adaptability to different size pipes. The same problem can be solved effectively when considering the

Research supported by National Natural Science Foundation of China (U1637207, 61673287) and National Science Foundation for Young Scientists of China (51705098).

Long Li, Peifeng Ma, Yichen Jiang, Tao Jin, Guangjie Yuan, and Yingzhong Tian are with School of Mechatronic Engineering and Automation, Shanghai University, Shanghai Key Laboratory of Intelligent Manufacturing and Robotics, Shanghai, 200444, China. (Yingzhong Tian is the corresponding author, troytian@shu.edu.cn)

Tong Wu is with Qian Xuesen Laboratory of Space Technology, China Academy of Space Technology, Beijing, 100094, and School of Mechatronic Engineering and Automation, Shanghai University, Shanghai, 200444, China

application of soft robot. In recent years, many experts and scholars at home and abroad have made relevant research and exploration in the field of flexible robots [10-12]. As in [11], by observing the leech, slugs and caterpillar peristalsis of the biological form, the authors proposed a longitudinal extensibility continuum robot, through the vacuum, and the use of three dc motor driven three hose actuators to realize three-dimensional (3D) climb movement. However, for longer complex pipe length, the device connected to the air source in the trachea has some limitations, due to the limited length of air tube restricts the scope of the robot's movement. For the worm-like robot in [12], the robot independently through before and after the end of the expansion of the airbag filling to realize fixed, moreover through the uniformly distributed in the middle of the three airbag filling deflated to realize 3D space within the scope of the telescopic peristalsis, but there is still a long distance movement of tracheal length is limited to the robot can't more disadvantages. In the above research paper, the existence of pneumatic layout makes the pipeline movement of the mechanism more complicated, and is not conducive to the production of software applied robot for practical application. In view of the above problems, this paper presents a three-hose actuator pipe crawling robot in the form of servo of the length of the trachea on the moving range of the robot.

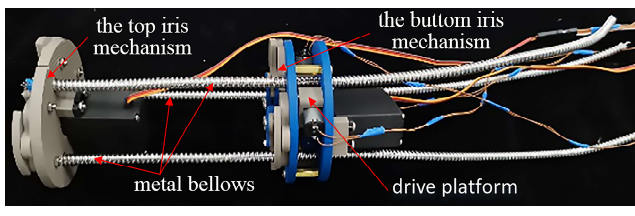
The details discussed in this paper are as follows: Firstly, proposed a tubular climbing robot induced by tri-tube soft actuators, and introduced its structure and manufacturing method in detail. Secondly, briefly introduce the working principle of pipeline crawling robot. Thirdly, based on the piecewise constant curvature theory, the kinematics model of three-hose actuator was established. Fourthly, built by the experimental adhesion measurement platform, we confirmed the inner diameter of the tube when the iris mechanism had the lowest pressure on the tube through the adhesion test, and carried out the vertical fixation experiment of the pipeline crawling robot under the tube of this size. It ensures that the robot can smoothly climb vertically in a water pipe with an inner diameter of 80-120 mm. Fifthly, pipe crawling robot was placed in different pipe diameters and bending angles to carry out the pipe crawling experiment. Finally, the paper summarizes the whole paper and looks forward to the future work.

## II. STRUCTURE AND MANUFACTURING METHOD

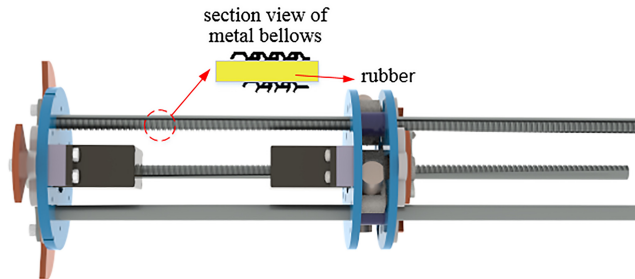
### A. Climbing Robot Structure

Taking leech's crawling behavior as inspiration, this paper designs three kinds of tubular crawling robots induced by flexible actuators and applies them to flex crawling with bent pipes. Leeches can twist their bodies by bending themselves, and they can use axial, radial, and oblique muscles to perform many of the body's functions, including elongation and bending. Taking advantage of the motion characteristics of the mechanism, it is considered that the motion of the mechanism cannot be realized by a single drive unit, so we divide the mechanism into two parts: the single-end fixed mechanism and the driving mechanism.

By imitating the movement of leech, we proposed a tubular crawling robot induced by a three-tube soft actuator, as shown in Fig. 1. In the crawling process, the movement of the retractable iris mechanism of the pipe robot can realize the fixation of the upper and lower ends of the robot, and the stretching, crawling and turning of the robot can be realized through the movement of the three-hose mechanism. Obviously, as can be seen from Fig. 1, the operation of our soft actuator is realized by the coordinated movement of three hoses. This is not entirely consistent with the actual movement of the leech. For example, our tubular robot cannot achieve radial size torsion. In addition, the way our robot is fixed is that after the diastolic iris mechanism moves, the slider squeezes the tube wall. When the extrusion pressure is large enough, the slider of the iris mechanism is relatively fixed with the wall of the tube. For the pipeline crawling robot, cornering is an index to measure its motion performance. Besides, in order to enhance the stiffness of the whole model, we insert the rubber rod into the metal bellows to enhance the support capability of the whole robot.



(a) Prototype of the robot

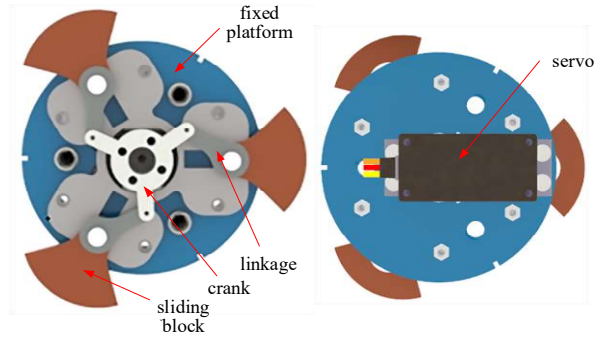


(b) 3D model of the robot

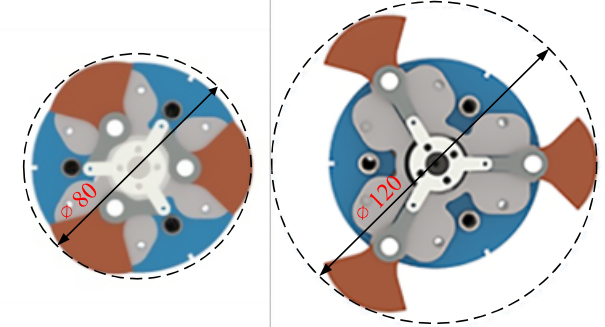
Fig. 1 The model of a tubular climbing robot induced by tri-tube soft actuators.

The size of iris mechanism installed at the front and rear end is shown in Fig. 2 (a), including a  $180^\circ$  servo (MG996R), a flat surface and three crank slider mechanisms. The servo and the crank are fixed connected by bolts. The rotation of the servo drives the slider to slide back and forth in the channel, thus realizing the opening and closing of the iris mechanism. In the closed state, the iris mechanism contour we designed is an 80mm circle, as shown in Fig. 2 (b). In the open state, the outer contour of the iris mechanism we designed is a 120mm circle, as shown in Fig. 2 (c). In other words, our three-tube soft-actuated tubular crawling robot can meet the crawling tasks of different pipes with the inner diameter of 80mm to 120mm. We coated the fan slider with a thin layer of silicone to improve the adhesion between the iris mechanism and the tube. An overall overview of the tri-tube soft actuators used to achieve telescopic crawling of a tubular crawling robot is shown in Fig. 3 (a).

They are a continuum part consisting of three parallel metal bellows. Three metal bellows pass through the reserved hole at the corresponding position on the drive platform at 120 degrees each other, and the drive platform is fixatedly



(a) Front view and rear view of iris mechanism



(b) Iris mechanism is folded

(c) Iris mechanism is unfolded

Fig. 2 Structure of iris mechanism and its unfolding and folding state.

connected with the upper end face of the iris mechanism at the bottom. Three DC motors (GA12-N20 reduction motor 12v Risym) are installed on the platform. One end of the metal bellows is fixed to the flat. Surface of the top iris mechanism and the other end is unrestrained. The gear connected on the output shaft of the DC motor meshes with the spiral groove on the surface of the metal bellows to form a mechanism similar to the rack and pinion, as shown in Fig. 3 (b). With the forward and reverse rotation of the motor, the whole drive platform together with the iris mechanism at the bottom can achieve linear movement up and down relative to the bellows. The continuous body can be bent and elongated with different directions and angles in three-dimensional spaces by changing the length of three metal bellows. The shape of the bellows is shown in Fig. 3 (c). It is made of spiral wound ribbon metal sheet with certain softness. The selected bellows have an outer diameter of 6mm and a minimum bending radius of 14mm. The reason we finally chose metal bellows over other materials is that they are made of spiral wound strips of metal with much better rigidity and support the iris mechanism at the top of the upper end.

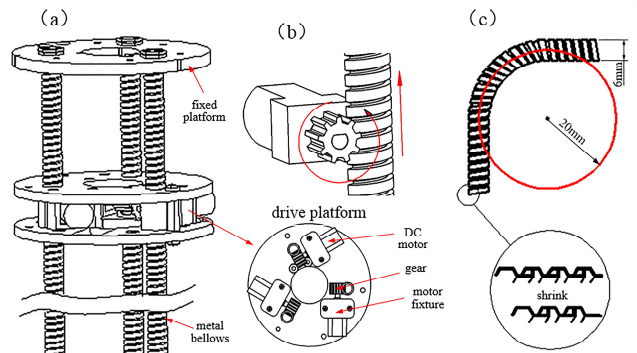


Fig. 3 Tri-tube soft actuators. (a) General overview of the tri-tube soft actuator. (b) Single tube driving method: motor-gear mechanism. (c) The maximum curvature of the metal bellows.

## B. Manufacturing Methods

For non-standard components of the mechanism, we use cheaper and lighter prints, which provide a good premise for bionics. Therefore, we use 3D (M200, Zortrax) to make the iris mechanism and the connecting parts of the driving platform. The selected material is lightweight and the printing effect is good ABS (Z-ABS, Zortrax) [13]-[14]. The connection between the groove and the fixed plate of the iris mechanism, and between the slider and the crank, are bolt and nut, which can improve the stability of the whole device.

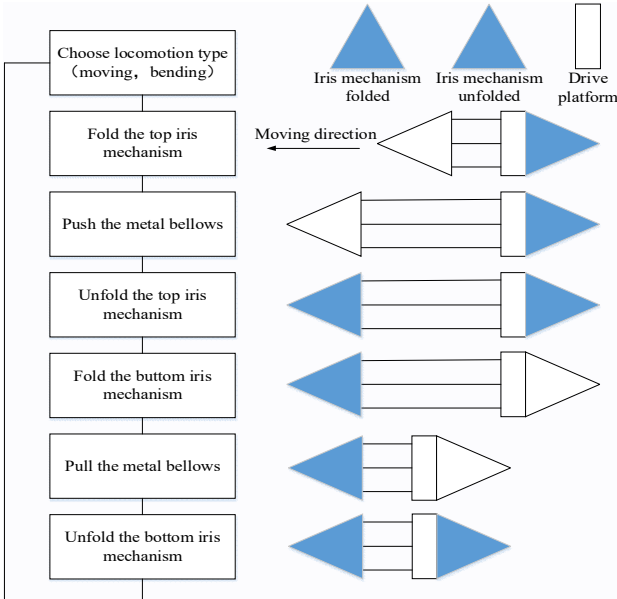


Fig. 4 The movement process diagram of the pipeline crawling robot.

## C. Mechanism Working Principle

The movement process of the robot is similar to the crawling process of leech, and its whole movement process is shown in Fig. 4. In the picture, the blue triangle represents the open iris mechanism, while the white triangle represents the closed iris mechanism, the white rectangle represents the driving platform, and the three horizontal lines represent the metal bellows. The overall movement flow is described as follows.

First of all, our pipe crawling robot needs to determine the type of movement, such as bending, forward and backward. After selecting the type of movement, we make the top iris mechanism close and separate it from the pipe wall, and then drive the motor in the plate to rotate and drive the three metal bellow tubes forward. When the three dc motors do not rotate at the same speed, the whole device turns to the side of the slower motor. When the top iris mechanism reaches the predetermined position, the top iris mechanism expands the inner wall of the main tube, and then another iris mechanism at the bottom closes and separates from the tube wall. The motor in the plate is then driven to rotate in the opposite direction, which drives the whole drive platform forward together with the iris mechanism at the bottom to complete a pipe crawling. For the feedback of motion control, we refer to genetic algorithm to optimize and improve the motion reliability of our pipeline robot [15].

## III. CALCULATION AND EXPERIMENT

### A. Kinematics Model with Constant Curvature

According to the piecewise constant curvature theory, the kinematics model of pipeline crawling robot is described by space mapping [16]. The homogeneous transformation matrix is used to describe the transformation of the soft robot from the base coordinate system to the end-effector coordinate system to obtain the end-pose of the robot. At the center of the base-plane iris mechanism, the corresponding base coordinates are established and the homogeneous transformation matrix is obtained by mapping the workspace. In Fig. 5, we established the kinematics model and obtained the coordinate system used to describe the terminal pose.

In the center of the iris institutions set up at the bottom of the base coordinate system, considering the  $Z_0$  base coordinate system axis direction and the robot's direction, variable  $\phi$  used to describe the robot end executor  $X_1$  axis and pedestal  $X_0$  axis is the direction of the deflection angle [17]. Meanwhile, the direction of  $Y_1$  is determined by the right-hand helix rule. Extend the  $X_1$  axis, the  $X_1$  shaft and base coordinate  $X_0Y_0$  - plane angle for  $\theta$ . In Fig. 4, when  $\phi = 0$ , by the main body of bending curvature of the model design, such as hose robot in  $X_0$  -  $Z_0$  plane, its body into a circular arc radius  $R$  [18]-[19]. To get the location of the end executor for  $p = [R(1-\cos\theta) \ 0 \ R\sin\theta]^T$  [20]. When there is a certain angle  $\phi$ , equal to rotation transformation of target parameters, namely,  $Z_0$  axis rotation around our base, the transformation matrix of the resulting from:

$$T = \begin{bmatrix} -2c\phi s^2 \frac{\theta}{2} + 1 & 2s\phi c\phi s^2 \frac{\theta}{2} & c\phi s\theta & \frac{c\phi(1-c\theta)}{k} \\ -2\phi c\phi s^2 \frac{\theta}{2} & -2c2\phi s^2 \frac{\theta}{2} + c\theta & s\phi s\theta & \frac{s\phi(1-s\theta)}{k} \\ -c\phi s\theta & -s\phi s\theta & c\theta & \frac{s\theta}{k} \\ 0 & 0 & 0 & 1 \end{bmatrix} \quad (1)$$

Where  $c\theta$  represents  $\cos\theta$ ,  $s\theta$  represents  $\sin\theta$ ,  $k$  for the pipeline model of constant curvature, bending the arc length of  $l$ , for the expression of  $\theta$  as  $\theta = kl$ , by the end of the transformation matrix to get actuator position coordinates of the origin for:

$$\begin{aligned} p_x &= \frac{\cos\phi(1-\cos\theta)}{k} \\ p_y &= \frac{\sin\phi(1-\cos\theta)}{k} \\ p_z &= \frac{\sin\theta}{k} \end{aligned} \quad (2)$$

The solution of the inverse kinematics equation obtained from the end position parameter and transformation matrix is:

$$\begin{aligned} a &= \frac{py^2}{pz^2 \sin\phi - 1} \\ \theta &= \arccos\left(\frac{1-a}{1+a}\right) \\ \phi &= \arctan\left(\frac{py}{px}\right) \end{aligned} \quad (3)$$

The space model of constant curvature kinematics we established is shown in Fig. 5.

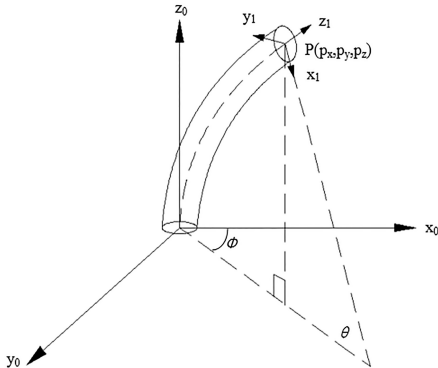


Fig. 5 Kinematic model of the bionic robot

By the calculation and analysis of the forward and inverse solutions of kinematics, the motion space of the hose robot can be determined by the determination of three parameters. The results of the forward and inverse kinematics solutions can be used as the input of the motion parameters of the three motors of the robot. Enable the mechanism to achieve straight or curved motion.

#### B. Adhesion Analysis of Iris Mechanism

Our pipe crawling robot uses the iris mechanism to attach the robot to achieve the fixation of the robot in the pipe, and our design requirements are applicable to the pipe with a diameter of 80~120mm, so the crank slider mechanism in the iris mechanism needs to be designed in size, as shown in Fig. 6.  $OA_1B_1$ ,  $OA_2B_2$  and  $OA_3B_3$  are three identical crank slider mechanisms used in our pipeline crawling robot. One of the crank slider mechanisms is selected for analysis [21-22]. In order to realize the climbing of the whole device in the pipeline, the torque  $M$  output by the servo to the crank must satisfy the following relationship:

$$\begin{aligned} F_1 \cos(\alpha) &= F \\ F_1 \sin(\alpha + \theta) \cdot l_1 &\leq M \\ F \cdot f &= mg \end{aligned} \quad (4)$$

Where  $m$  is the mass of the whole device,  $F_1$  is the force on the connecting rod  $A_1B_1$ ,  $\alpha$  is the angle between  $OA_1$  and  $A_1B_1$ ,  $\theta$  is the angle between  $OB_1$  and  $OA_1$ ,  $l_1$  and  $l_2$  respectively represent the length of crank  $OB_1$  and connecting rod  $A_1B_1$ .

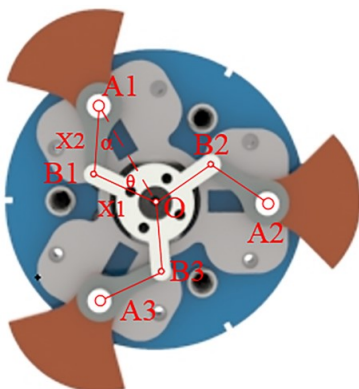


Fig. 6 Dimension design of crank slider mechanism

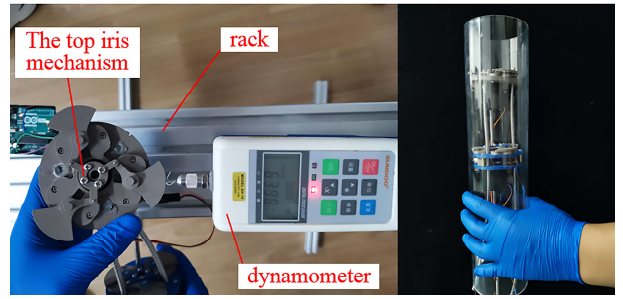


Fig. 7 Adhesion test and vertical fixation test

Due to the limitation of the three metal bellows, the structure of the crank slider itself and the motion range of the slider, we selected the crank and the connecting rod to have the same length and to be in a collinear state when the iris mechanism is fully developed.  $l_1$  in the Fig. 6 is equal to  $l_2$ , and the angle  $\alpha$  is the same as angle  $\theta$ . From this we can get the relationship between torque  $M$  and angle  $\theta$ .

$$\frac{mg \sin(2\theta)}{f \cos \theta} \cdot l_2 = \frac{2mg \sin \theta}{f} \cdot l_2 \leq M \quad (5)$$

Obviously,  $\theta$  is at its maximum when the iris mechanism is fully closed (less than 90 degrees), at this moment the required crank torque  $M$  is at its maximum.

#### A. Adhesion Test

FIG. 7 (a) shows the adhesion test experiment. The specific test method is as follows: First of all, we put the servo, which is fixed on the iris mechanism in the state of stall rotation with different rotation angles, and then record the reading of a dynamometer When the steering gear is squeezed by the force meter on the screw, and take this number as the maximum output pressure of the iris mechanism. After a series of tests, we can obtain the diagram of the change of the output pressure with the different rotation angle of the iris mechanism as showing in Fig. 8.

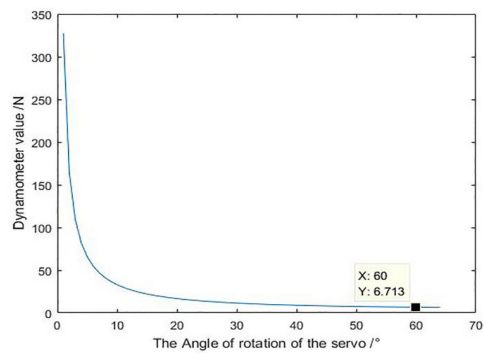


Fig. 8 The value of the dynamometer varies with the angle of the servo

As can be seen from Fig. 8, the degree of rotation of the servo corresponding to the minimum output pressure of iris mechanism is about 60 degrees. At this time, the outer contour diameter of the iris mechanism is 90 mm. Since the friction coefficient between the tube and the silica gel on the surface of the iris mechanism is difficult to be measured, We placed the device in a PVC tube with an inner diameter of 90 mm for test experiments, as shown in Fig. 7(b), which showed that the iris mechanism could make the robot vertically fixed in a 90mm pipe, thus confirming that our

robot could realize vertical crawling in a pipe with an inner diameter of 80-120mm.

### C. Creep Experiment

In order to verify that our designed pipe crawling robot can adapt to different pipe diameters and bending angles, we placed the robot in a pipe with a preset size for crawling experiment. Three kinds of pipelines with inner diameters of 90 mm, 105 mm and 120 mm were selected for the crawling experiment of straight line and bending, and the motion of the robot was controlled by the motor.

The experimental results are shown in Fig. 9 (a). In addition, we asked the robot to perform cornering crawling experiments in 45° and 90° common curved pipes. The experimental results are shown in Fig. 9 (b).

### IV. CONCLUSION

In this work, we presented the design analysis and fabrication of a novel pipe crawling robot, which is guided by tri-tube soft actuation and fixed to pipe by iris mechanism. The tri-tube soft actuation composed by the normal hose used in our home can be driven by three dc motors in the mode like the gear and rack. The iris mechanism made of three crank slider mechanism can be actuated by one servo symmetrically. The analysis based on equal curvature hypothesis and experiments showed the robot can bend to 90 degrees easily, which verified the guiding function in different curved pipes. In order to analyze, the iris mechanism is divided into three crank slider mechanism. Both the analysis and experiments display the friction force is enough to hold the weight of the robot. Therefore, our robot can be working in various pipe lines in the 3D space. Although our robot features a soft characteristic, the crawling motion do not need air source and air tube usually applied in the soft robotics field, which shows the resolution of problems in the combination of the soft structure and the crawling robot without operation space limitation.

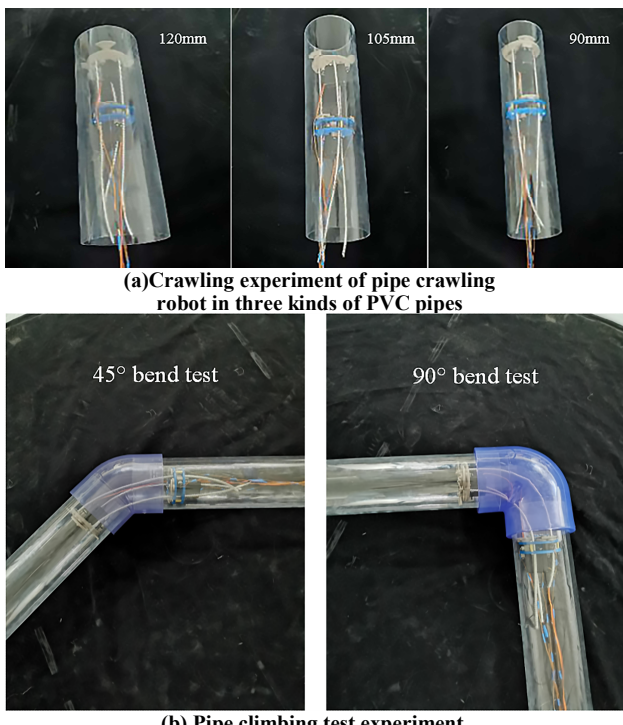


Fig. 9 Two kinds of pipe bending crawling experiments with different bending angles

At present, our control circuit is still placed outside the three-hose actuated pipeline robot. In the future, we will reduce the size of the control circuit and install it on the mobile robot body to dissolve the limitation of the pipeline robot completely. In addition, we will install a camera on the head of the mobile robot and send the internal situation of the pipe back to the computer for pipe inspection.

### V. REFERENCES

- [1] Zheng shiyu, "Overview of research status of soft robot," *Equipment management and maintenance*, 2018(02): 38-39.
- [2] Wu zhonghai, "Design and system analysis of pipeline inspection robot," *Electronic technology and software engineering*, 2019(16): 121-122.
- [3] Tao chen, Qiongfeng Shi, Minglu Zhu, Tianyi He, Lining Sun, Lei Yang, Chengkuo Lee, "Triboelectric Self-Powered Wearable Flexible Patch as 3D Motion Control Interface for Robotic Manipulator," *ACS Nano*, 2018, 12, 11, 11561-11571.
- [4] Tao Chen, Mingyue Zhao, Qiongfeng Shi, Zhan Yang, Huicong Liu, Lining Sun, Jianyong Ouyang, and Chengkuo Lee, "Novel Augmented Reality Interface Using A Self-Powered Triboelectric Based Virtual Reality 3D-Control Sensor," *Nano Energy*. 2018, 51, 162-172.
- [5] Hou taogang, wang tianmiao, su haohong, chang shuai, Chen lingkun, hao yufei, wen li, "Software robot cutting-edge technology and application hotspots," *Science and Technology Herald*, 2017, 35(18): 20-28.
- [6] Zheng haibin, "Flexible pipeline inspection robot based on Internet of things," *Communication Power Technology*, 2019, 36(01): 269-270.
- [7] Xiao Yao-Yu, Jiang Zhi-Chao, Tong Xia, Zhao Yue, "Biomimetic Locomotion of Electrically Powered "Janus" Soft Robots Using a Liquid Crystal Polymer," *Advanced Materials* (Deerfield Beach, Fla.), 2019, 31(36).
- [8] Oliver Jeremie D, DeLoughery Emma P, "Leeches and Plastic Surgery in the Modern Era," *Plastic Surgical Nursing* : official journal of the American Society of Plastic and Reconstructive Surgical Nurses, 2019, 39(3).
- [9] Sangbae Kim, Cecilia Laschi, Barry Trimmer, "Soft robotics: a bioinspired evolution in robotics," *Trends in Biotechnology*, 2013, 31(5).
- [10] Long Li, Tao Jin, Fei Yang, Yingzhong Tian, Yang Xian, and Fengfeng Xi, "Design and Analysis of a Square-shaped Continuum Robot with Better Grasping Ability," *IEEE ACCESS*, 2019, 7: 57151-57162.
- [11] Kanada Ayato, Giardina Fabio, Howison Toby, Mashimo Tomoaki, Iida Fumiya, "Reachability Improvement of a Climbing Robot Based on Large Deformations Induced by Tri-Tube Soft Actuators," *Soft Robotics*, 2019, 6(4)
- [12] Zhang Boyu, Fan Yingwei, Yang Penghui, Cao Tianle, Liao Hongen, "Worm-Like Soft Robot for Complicated Tubular Environments," *Soft robotics*, 2019, 6(3).
- [13] M. M. Porter et al, "3D-printing and mechanics of bio-inspired articulated and multi-material structures," *Journal of the Mechanical Behavior of Biomedical Materials*, Article vol. 73, pp. 114-126, Sep 2017.
- [14] N. W. Bartlett et al, "A 3D-printed, functionally graded soft robot powered by combustion," *Science*, Article vol. 349, no. 6244, pp. 161-165, Jul 2015.
- [15] Zhang Q, Dong Y, Peng Y, et al. "Asymmetric Bouc-Wen hysteresis modeling and inverse compensation for piezoelectric actuator via a genetic algorithm-based particle swarm optimization identification algorithm," *Journal of Intelligent Material Systems and Structures*, 2019, 30(8): 1263-1275.
- [16] Cai Jianguo, Zhang Qian, Feng Jian, Xu Yixiang, "Modeling and Kinematic Path Selection of Retractable Kirigami Roof Structures," *Computer-Aided Civil and Infrastructure Engineering*, 2019, 34(4): 352-363.

- [17] Y. Tian, M. Luan, X. Gao, W. Wang, and L. Li, "Kinematic analysis of continuum robot consisted of driven flexible rods," *Math. Probl. Eng.*, vol. 2016, 2016.
- [18] Jiang guoping, meng fanchang, shen jingjin, xu fengyu, "Overview of kinematics and dynamics modeling of soft robots," *Journal of Nanjing university of posts and telecommunications* (natural science edition), 2018, 38(01): 20-26.
- [19] Zhao wenqiang, zhang xiaojun, miao Yang, "Kinematics analysis and simulation of KUKA robot based on MATLAB," *Mechanical Research and Application*, 2019, 32(04): 1-5+11.
- [20] Xu fengyu, meng fanchang, fan baojie, peng gaoliang, shen jingjin, jiang guoping, "Research review on software robot drive, modeling and application," *Journal of Nanjing university of posts and telecommunications* (natural science edition), 2019, 39(03): 64-75.
- [21] Wen li, wang hesheng, "Research prospect of soft robot: structure, drive and control," *Robot*, 2018, 40(05): 577.
- [22] Cai Jianguo, Yang Ruiguo, Wang Xinyu, Feng Jian, "Effect of Initial Imperfections of Struts on the Mechanical Behavior of Tensegrity Structures," *Composite Structures*, 2019, 207: 871-876.